

Optimal control of quantum revival

Esa Räsänen^{1,2,3} and Eric J. Heller^{3,4}

¹ Department of Physics, Tampere University of Technology, FI-33101 Tampere, Finland

² Nanoscience Center, Department of Physics, University of Jyväskylä, FI-40014 Jyväskylä, Finland

³ Physics Department, Harvard University, Cambridge, Massachusetts 02138, USA

⁴ Department of Chemistry and Chemical Biology, Harvard University, Cambridge, Massachusetts 02138, USA

Received: date / Revised version: date

Abstract. Increasing fidelity is the ultimate challenge of quantum information technology. In addition to decoherence and dissipation, fidelity is affected by internal imperfections such as impurities in the system. Here we show that the quality of quantum revival, i.e., periodic recurrence in the time evolution, can be restored almost completely by coupling the distorted system to an external field obtained from quantum optimal control theory. We demonstrate the procedure with wave-packet calculations in both one- and two-dimensional quantum wells, and analyze the required physical characteristics of the control field. Our results generally show that the inherent dynamics of a quantum system can be idealized at an extremely low cost.

PACS. XX.XX.XX No PACS code given

1 Introduction

Quantum revival, i.e., periodic recurrence of a wave function is a fundamental property of a time-dependent quantum system. The quality of the quantum revival can be determined by a simple overlap between the initial and final states after the *ideal* revival time, i.e., the revival time of the unperturbed system. In this respect, the quality corresponds to quantum fidelity [1].

Fidelity is the most important measure of the functionality of a quantum information device, and in this respect it has been subjected to extensive theoretical work [2]. In experiments fidelity is greatly affected not only by eventual decoherence and dissipation due to the coupling with the environment, but also by internal imperfections such as random irregularities and impurities. The standard approach to overcome this problem is to increase the sample quality or to make it, by other means, particularly resistant to imperfections.

An alternative strategy to improve fidelity, which is the topic of this work, is to couple the system to an external *control field* that assists the system to overcome and/or to compensate the effects induced by irregularities. Such scenarios have attracted significant interest in the design of high-fidelity quantum gates in optical lattices [3]. Here we show that optimizing the control field with quantum optimal control theory [4, 5] (OCT) leads to a practically complete restoration of the fidelity and thus to the full quantum revival even at significantly low energies of the control field. We analyze in detail the properties of the optimized field and demonstrate the scheme for the time

evolution of one- and two-dimensional wave packets, respectively. Our findings have broader applicability to general control problems, where the inherent dynamics can be assisted by optimized fields subject to strict constraints in terms of the intensity and the frequency range.

2 Optimal control theory

Since its formulation [4, 5] in the 1980s OCT has increased its popularity in chemistry and condensed matter physics [6]. The central idea of OCT is to replace trial-and-error type learning-loop experiments with a rigorous extension of the classical control problem to quantum mechanics. In all OCT applications the objective is to find an external time-dependent field $\epsilon(t)$ that drives the system to the predefined target, e.g., to a certain quantum state, through the solution of the Schrödinger equation,

$$i \frac{\partial}{\partial t} \Psi(\mathbf{r}, t) = \left[\hat{T} + \hat{V} - \hat{\mu} \epsilon(t) \right] \Psi(\mathbf{r}, t), \quad (1)$$

where dipole approximation is applied with $\hat{\mu} = -\mathbf{r}$ (Hartree atomic units used throughout). The central idea is to maximize the target functional

$$J_1[\psi] = \left\langle \Psi(\mathbf{r}, T) | \hat{O} | \Psi(\mathbf{r}, T) \right\rangle, \quad (2)$$

at time $t = T$. In this study we consider two types of target operators: (i) projection operator $\hat{O} = |\Phi_F\rangle \langle \Phi_F|$ with Φ_F as our target *state*, and (ii) a local operator $\hat{O} = \rho_F(\mathbf{r})$

representing our target *density* at $t = T$. The maximum value obtained for J_1 is referred to the *yield*.

The optimized pulse is exposed to two important constraints. First, the fluence, i.e., the time-integrated intensity F_0 is kept fixed by applying a functional,

$$J_2[\epsilon] = -\alpha \left[\int_0^T dt \epsilon^2(t) - F_0 \right], \quad (3)$$

where α is a time-independent Lagrange multiplier. Secondly, a spectral filter is applied to cut off the highest frequencies, e.g., unrealistic photon energies. This is done by multiplying the Fourier-transformed pulse by a filter function $f(\omega)$, that represents the desired frequency range. Thereafter, an inverse Fourier transform of the product is taken to obtain the time-resolved filtered pulse (see Ref. [7] for details).

Finally, the time-dependent Schrödinger equation [Eq. (1)] must be satisfied in the control procedure. This gives us yet another functional,

$$J_3[\epsilon, \Psi, \chi] = -2 \operatorname{Im} \int_0^T \langle \chi(t) | i\partial_t - \hat{H}(t) | \Psi(t) \rangle, \quad (4)$$

where the auxiliary function $\chi(t)$ can be regarded as a time-dependent Lagrange multiplier [4].

Variation of the total functional $J = J_1 + J_2 + J_3$ with respect to Ψ , χ , ϵ , and α leads to the control equations

$$i\partial_t \Psi(t) = \hat{H}(t) \Psi(t), \quad \Psi(0) = \Phi_I, \quad (5)$$

$$i\partial_t \chi(t) = \hat{H}(t) \chi(t), \quad \chi(T) = \hat{O} \Psi(T), \quad (6)$$

$$\epsilon(t) = -\frac{1}{\alpha} \operatorname{Im} \langle \chi(t) | \mu | \Psi(t) \rangle, \quad (7)$$

$$\int_0^T dt \epsilon^2(t) = F_0. \quad (8)$$

which are solved iteratively [8,7] by applying here the forward-backward propagation scheme of Werschnik and Gross [9]. Typically a converged field is obtained within 100...300 OCT iterations. We have applied `octopus` code [10] in all the calculations.

3 Results

3.1 Superposition in a one-dimensional well

We start by considering a single particle with mass $m = 1$ in a one-dimensional square quantum well with infinite boundaries and a length $L = 20$. The energy eigenstates are given by $E_n = \pi^2 n^2 / (2mL^2) = (\pi^2/800)n^2$ with $n = 1, 2, \dots$. By expanding the wave function and equalizing the phase factors it is straightforward to show [11,12,13] that the exact quantal revival time for *any* wave function is given by $T_{\text{rev}} = 4mL^2/\pi = 1600/\pi$. However, if the wave function is a superposition of two eigenstates with E_n and E_m , the first full revival occurs already at $T_{\text{rev}}^{mn} = 2\pi/(E_m - E_n)$.

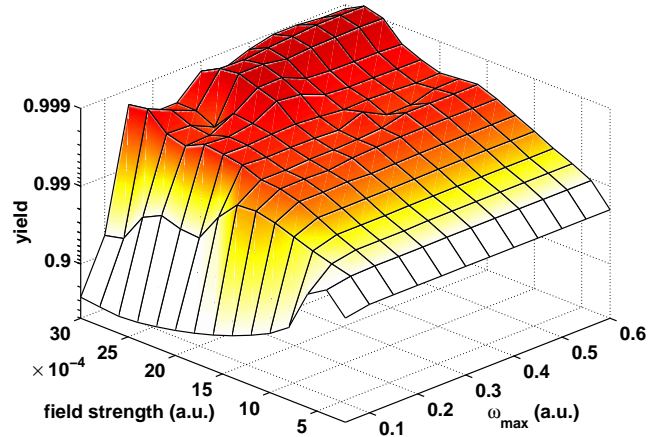


Fig. 1. (color online) Yield as a function of the field strength and maximum frequency ω_{max} of the optimized field in a revival process of a one-dimensional square quantum well distorted by a Gaussian impurity. The initial state is a superposition of the two lowest eigenstates in a clean system.

In our first example our initial state is a superposition of the lowest two eigenstates, so that the first revival time with $|\langle \Psi(x, T_{\text{rev}}) | \Psi(x, 0) \rangle|^2 = 1$ is $T_{\text{rev}}^{12} = T_{\text{rev}}/3 = 1600/(3\pi)$. Starting from the *same state* but supplying our quantum well with a Gaussian impurity $V_{\text{imp}}(x) = \beta \exp[-(x - x_0)^2/\gamma^2]$ with $\beta = 0.1$, $\gamma = 1$, and $x_0 = 2.5$ leads to a reduced overlap, $|\langle \Psi'(x, T_{\text{rev}}) | \Psi(x, 0) \rangle|^2 = 95.9\%$. Here $|\Psi'\rangle$ and $|\Psi\rangle$ correspond to distorted and clean systems, respectively.

Our task now is to restore the full quantum revival by optimizing a control field with a target $\Phi_F = \Psi(x, 0) = \Psi(x, T)$. Figure 1 shows the obtained yield (overlap) as a function of the maximum allowed frequency ω_{max} and the field strength of the initial constant field ϵ (so that the fluence $F_0 = T_{\text{rev}}\epsilon^2$ is kept fixed in the OCT procedure). Generally, Fig. 1 demonstrates that the optimization works in the desired manner, so that we find a significant increase in the yield even up to $> 99.9\%$. The price to pay is embedded in the allowed intensity and frequency of the field as analyzed in the following.

As shown in Fig. 1 the yield is strongly increased when ω_{max} is increased above ~ 0.15 . It can be expected that the "critical" frequency is related with the energy gaps in the spectrum. Now the critical frequency is clearly above the first few energy gaps, so it seems likely that (de-)excitations at relatively high levels are needed in the distorted system to produce a high overlap with the initial state. The coupling with the optimized field with the energy levels is studied in more detail in Sec. 3.2. We point out that at small cutoff frequencies ($\omega_{\text{max}} \lesssim 0.15$) the yield is smaller than in the distorted system *without* a control field; with a limited frequency range, and especially when supplied with a high field strength, the field is causing harm in the system despite the optimization.

In a reasonable frequency range, the required fluence to reach a high overlap is very small. For example, 99%

yield can be obtained with $F_0 \sim 2 \times 10^{-3}$, which is only about 5% of the first excitation energy $E_1 - E_0 = 0.037$. The energy carried by the field is also much smaller than the difference in the energy levels of the system with and without the impurity. Furthermore, in conventional control problems where, e.g., charge transfer or a desired excitation is optimized, the typical intensities are larger by several orders of magnitude despite similar system characteristics [14,15,16]. Overall, we may conclude that in processes where the inherent dynamics gives a high initial overlap (as in the partial revival), OCT finds the route to almost 100% yield with an extremely low price.

3.2 Gaussian packet in a one-dimensional well

Next we study the revival of a Gaussian wave packet in the same one-dimensional quantum well. The wave packet is defined as $\Psi(x, 0) = \exp(-(x + x_0)^2)/\sqrt{\pi}$ with $x_0 = -3\sqrt{3}$, and the impurity is the same as before [see the inset of Fig. 2(d)]. As the wave packet consists of a large ensemble of eigenstates the first revival will occur at the universal revival time $T_{\text{rev}} = 1600/\pi$ as discussed in the previous section. This is set as the time of the control field, and the target is now the (single-particle) density $\rho_{\text{F}}(x, T = T_{\text{rev}}) = |\Psi(x, 0)|^2$.

Figure 2 summarizes the OCT results obtained with a threshold frequency $\omega_{\text{max}} = 1$ and fluence $F_0 = 0.00203$. Figure 2(a) shows the overlap with the initial wave packet as a function of time in the case of (i) a clean system (solid line), (ii) a distorted system with the impurity (dotted line), and (iii) a distorted but controlled system (dashed line). During the last stages of the propagation [Fig. 2(c)] the controlled wave packet closely follows the ideal system and reaches 99.9% overlap, whereas the uncontrolled evolution leads to about 88%. Thus, the optimization seems to find the correct “path” in time, so that the field continuously corrects the evolution toward the ideal one, even though the target functional is *not* time-dependent.

The optimized control field and its Fourier spectrum are shown in Figs. 2(b) and (d), respectively. The strongest two peaks in the spectrum at $\omega = 0.025 \dots 0.05$ correspond to the transition between the first two levels with $\Delta E = 0.037$, and the peak at $\omega \sim 0.15$ is likely to correspond to the transition between the 5th and 6th states with $\Delta E = 0.13$. Figure 2(e) shows the projections of the propagated single-electron orbitals (of the system with an impurity and a control field) to the initial orbitals (of the clean system). Here the excitation processes between the 1st and the 2nd, and, on the other hand, between the 5th and the 6th states are clearly visible. At the end of the pulse the initial occupations are reached as the initial wave packet is reconstructed in the controlled revival process.

In Fig. 3 we show the effect of the field strength and the maximum allowed frequency on the obtained yield in the controlled revival of a Gaussian wave packet. The critical field strength (of the initial constant field) to reach a yield close to 0.999 – after the optimization within a fixed fluence – is $\epsilon \sim 1.2 \times 10^{-3}$ corresponding to $F_0 \sim 0.00073$. As a function of ω_{max} we find two steps at around

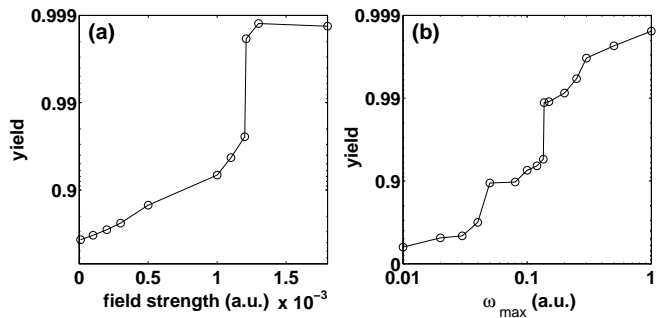


Fig. 3. Yield in the controlled revival of a one-dimensional Gaussian wave packet as a function of (a) the field strength (without a filter, i.e., $\omega_{\text{max}} \rightarrow \infty$) and (b) the maximum allowed frequency when the field strength of the initial pulse is $\epsilon = 0.002$.

0.004...0.005 and 0.15, respectively. They correspond to the excitations $1 \leftrightarrow 2$ and $5 \leftrightarrow 6$ and confirm the importance of those processes in the controlled evolution.

Next we consider the effect of the impurity characteristics on the controllability. It is expected that a narrow impurity as the one in our example [inset of Fig. 2(d)] probes higher excitations than a broader impurity, and hence the dynamics and control procedure are qualitatively different in those cases. To test this, we increase the width parameter γ of the Gaussian impurity from 1 to 3 in $V_{\text{imp}}(x)$ (see Sec. 3.1) and decrease the height β from 0.3 to 0.2. This change reduces the quality of the revival from 88% to 80%. However, there is no significant change in the control process: the yields are generally comparable, and the step in Fig. 3(a) is at the same place. The yield as a function of the threshold frequency is also similar, although the step structure is not so prominent.

3.3 Gaussian packet in a two-dimensional well

Finally we move our attention to a two-dimensional example. This extends the physical relevance of the proposed scheme to two-dimensional electron gases having a variety of applications in, e.g., quantum Hall and quantum dot physics [17]. We consider a square quantum well with hard-wall boundaries and side length $L = 12$ [see Fig. 4(a)]. The initial Gaussian wave packet is given by $\Psi(x, y, 0) = \delta \exp(-(x + x_0)^2 + (y + y_0)^2)/(2\delta^2)$ with $\delta = 0.7$, $x_0 = 1$, and $y_0 = 2$. We note that due to symmetry the wave-packet propagation is separable to x and y components. However, we expose the system to ten *random* repulsive impurities visualized in Fig. 4(b) (two of them merged together), so that the problem is no longer separable.

Time-evolution of the wave packet in the distorted potential leads to 71% revival quality. The overlap as a function of time is shown in Fig. 5(a). To correct the process we add a control field with two independent components polarized in x and y directions, respectively. As in the previous example, the target is the density of the initial (single-electron) wave packet at $t = T = T_{\text{rev}}$. The total

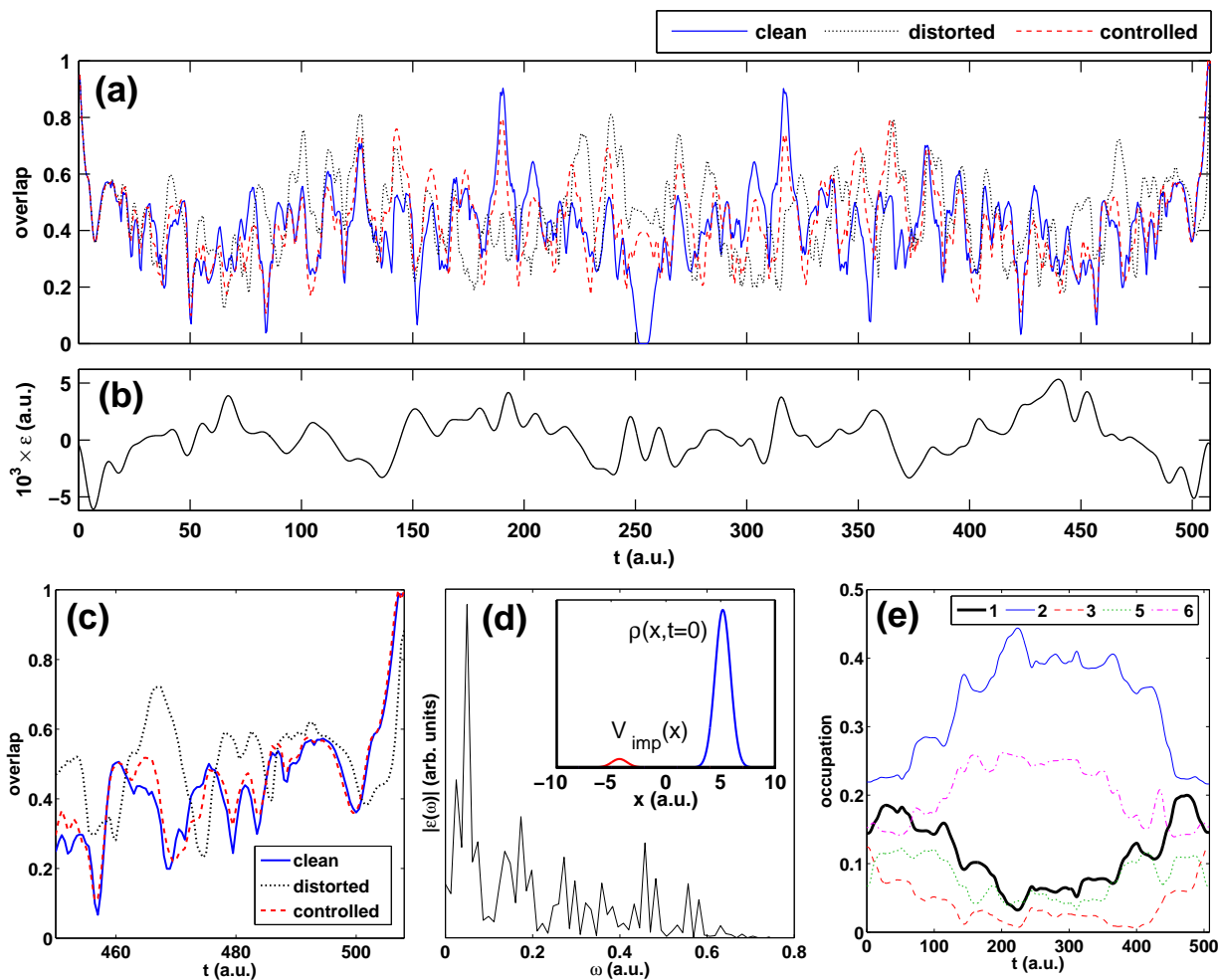


Fig. 2. (color online) Controlled revival of a one-dimensional wave packet in a square quantum well. (a) Time-dependent overlap of the propagated wave packet with the initial one in a clean system (solid lines), in a distorted system (dotted lines), and in a distorted by controlled system (dashed lines). In (c) the last part of the propagation is zoomed. (b) Optimized control field. (d) Fourier spectrum of the control field. The inset shows the external potential with the initial wave packet and the impurity. (e) Projections of the propagated single-electron orbitals to the initial ones. The maximum allowed frequency is $\omega_{\max} = 1$ and the fluence is fixed to $F_0 = 0.00203$.

field fluence is fixed to $F_0 = 0.07348$ and the maximum frequency allowed in the optimization is $\omega_{\max} = 0.5$. With these constraints OCT produces a control field shown in Fig. 5(b) that drives the system to 97% overlap. Thus, the control procedure works well also in a two-dimensional system.

Figures 4(c-e) show the single-electron densities during the time evolution at a half of the revival time $T/2$, at $3T/4$, and at the revival time T . Interestingly, at $T/2$ the distorted packet is rather close to the ideal one as shown as a high overlap in Fig. 5(a). Towards the end of the evolution, however, the controlled procedure starts to resemble the ideal one, whereas the distorted process becomes very different. Hence, it seems that the essential adjustments in the controlled evolution always occur during the last stages of the process. The relevance of the earlier stages in the “system preparation” could be studied by considering *partial* control fields affecting the system only during,

e.g., the last 10% of the time evolution. In addition, it would be worthwhile to examine if the ideal evolution (in a clean system) can be followed *continuously in time* by applying a time-dependent target functional [7]. These issues are beyond the scope of the present study and subject to future research.

Finally we comment on the simplification of using a fixed and static impurity configurations in the above examples. The obtained control field is found only for a specific configuration; a general field able to control a large ensemble of potentials would be impossible to find in practice. Nevertheless, we point out there are several physical situations, e.g., in semiconductor heterostructures, where the impurity configuration in a given experimental setup can be found. For example, in a quantum-dot experiment in Ref. [18] the size and position of a migrated impurity ion was accurately determined in a system that was otherwise close to an ideal two-dimensional harmonic oscil-

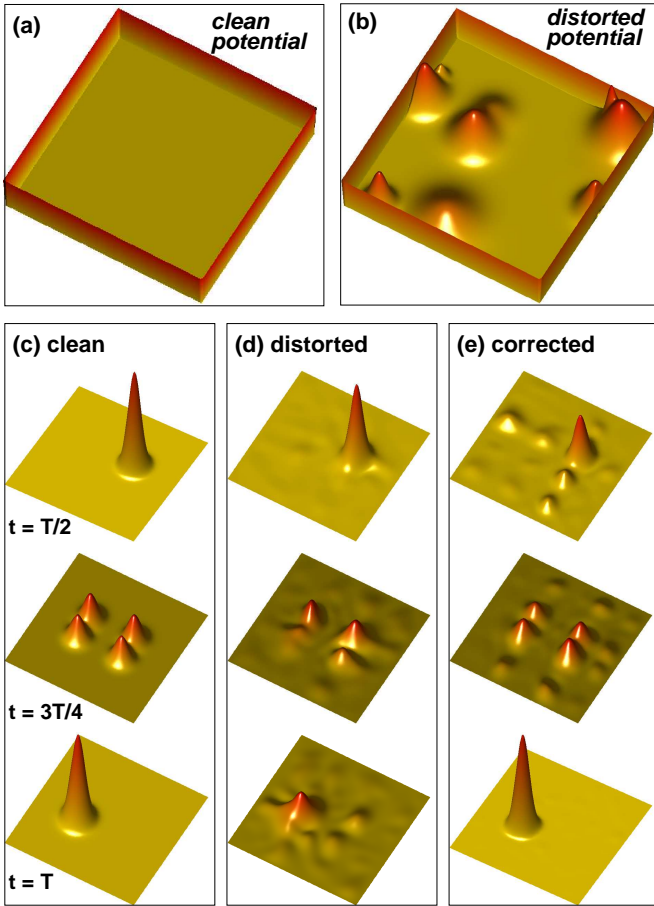


Fig. 4. (color online) (a-b) External potentials of clean and distorted square quantum wells, respectively. (c-e) Single-electron densities at times $t = T/2$, $3T/4$, and T of the propagation in a clean, distorted, and controlled system, respectively.

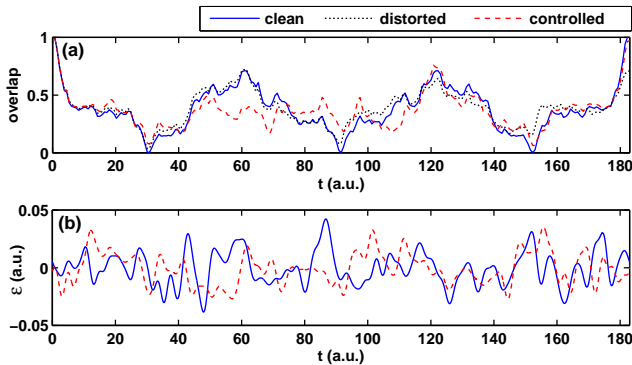


Fig. 5. (color online) (a) Overlap as a function of time in a revival process of a two-dimensional Gaussian wave packet in a square quantum well. (b) Optimized two-component (x and y) control field leading to 97% overlap. Here $F_0 = 0.07348$ and $\omega_{\max} = 0.5$.

lator. In such a situation, the Hamiltonian is known and optimization of the field to obtain a predefined target is possible.

4 Summary

To summarize, we have analyzed quantum revival processes of single-particle states and Gaussian wave packets in one- and two-dimensional quantum wells. We have shown that the quality of the quantum revival in a realistic (distorted) system can be greatly improved by coupling the system to an external control field. The control field can be optimized with quantum optimal control theory to maximize the overlap between the initial wave function and the time-propagated one at the revival time – within predefined constraints on the fluence and maximum allowed frequency. We have analyzed how the field constraints affect the obtained yields, and found that very low intensities are sufficient to obtain yields above 99% in one-dimensional systems. The threshold frequencies to achieve high yields can be associated with excitation energies in the system. Our procedure has broader implications to general control problems, where the objective is to supplement the inherent dynamics disrupted by irregularities. The demonstrated applicability to two dimensions shows that the proposed approach could be used to increase quantum fidelity in, e.g., quantum Hall devices.

This work was supported by the Academy of Finland, the Wihuri Foundation, and the Magnus Ehrnrooth Foundation. CSC Scientific Computing Ltd. is acknowledged for computational resources.

References

1. T. Gorin, T. Prosen, T. H. Seligman, and M. Znidaric, *Phys. Rep.* **435**, 33 (2006).
2. For a review, see, e.g., S. Kohler and P. Hänggi, *Fortschr. Phys.* **54**, 804 (2006).
3. See, e.g., B. Khani, S. T. Merkel, F. Motzoi, Jay M. Gambetta, and F. K. Wilhelm, *Phys. Rev. A* **85**, 022306 (2012) and references therein.
4. A. P. Peirce, M. A. Dahleh, and H. Rabitz, *Phys. Rev. A* **37**, 4950 (1988);
5. R. Kosloff, S. A. Rice, P. Gaspard, S. Tersigni, and D. J. Tannor, *Chem. Phys.* **139**, 201 (1989).
6. C. Brif, R. Chakrabarti, and H. Rabitz, *New J. Phys.* **12**, 075008 (2010).
7. For a review, see, e.g., J. Werschnik and E. K. U. Gross, *J. Phys. B: Atom. Mol. Opt. Phys.* **40**, R175 (2007).
8. W. Zhu and H. Rabitz, *J. Chem. Phys.* **108**, 1953 (1998); **109**, 385 (1998).
9. J. Werschnik and E. K. U. Gross, *J. Opt. B: Quantum Semiclass. Opt.* **7**, S300 (2005).
10. M. A. L. Marques, A. Castro, G. F. Bertsch and A. Rubio, *Comp. Phys. Comm.* **151**, 60 (2003); A. Castro, H. Appel, M. Oliveira, C. A. Rozzi, X. Andrade, F. Lorenzen, M. A.

- L. Marques, E. K. U. Gross, and A. Rubio, *Phys. Stat. Sol. (b)* **243**, 2465 (2006).
11. R. Bluhm, V. A. Kostelecky, and J. A. Porter, *Am. J. Phys.* **64**, 944 (1996).
 12. D. L. Aronstein and C. R. Stroud, *Phys. Rev. A* **55**, 4526 (1997).
 13. D. F. Styer, *Am. J. Phys.* **69**, 56 (2001).
 14. A. Putaja and E. Räsänen, *Phys. Rev. B* **82**, 165336 (2010).
 15. E. Räsänen, A. Castro, J. Werschnik, A. Rubio, and E. K. U. Gross, *Phys. Rev. B* **77**, 085324 (2008).
 16. E. Räsänen, A. Castro, J. Werschnik, A. Rubio, and E. K. U. Gross, *Phys. Rev. Lett.* **98**, 157404 (2007).
 17. L. P. Kouwenhoven, D. G. Austing, and S. Tarucha, *Rep. Prog. Phys.* **64**, 701 (2001); S. M. Reimann and M. Manninen, *Rev. Mod. Phys.* **74**, 1283 (2002).
 18. E. Räsänen, J. Könemann, R. J. Haug, M. J. Puska, and R. M. Nieminen, *Phys. Rev. B* **70**, 115308 (2004).